A VARIATIONAL PANSHARPENING APPROACH BASED ON REPRODUCIBLE KERNEL HILBERT SPACE AND HEAVISIDE FUNCTION

Liang-Jian Deng [1], *Gemine Vivone* [2], *Weihong Guo* [3], *Mauro Dalla Mura* [4], *Jocelyn Chanussot* [4]

[1] School of Mathematical Sciences, University of Electronic Science and Technology of China, Chengdu, Sichuan, 611731, China
[2] North Atlantic Treaty Organization (NATO) Science & Technology Organization (STO) Centre for Maritime Research and Experimentation (CMRE), La Spezia, Italy
[3] Case Western Reserve University, Cleveland, OH, 44106, USA
[4] University of Grenoble Alpes, CNRS, GIPSA-lab, F-38000 Grenoble, France

ABSTRACT

In this paper, we propose a continuous modeling and sparse optimization based method for the fusion of a panchromatic (PAN) image and a multispectral (MS) image. The proposed model is mainly based on reproducing kernel Hilbert space (RKHS) and approximated Heaviside function (AHF). In addition, we also design an iterative strategy to recover more image details. The final model is a convex one and solved by the designed alternating direction method of multipliers (ADMM) which guarantees the convergence of the proposed method. Experimental results on two real datasets corresponding to different sensors and different resolutions demonstrate the effectiveness of the proposed approach as compared with several state-of-the-art pansharpening approaches.

1. INTRODUCTION

Pahsharpening is a technique that fuses a *high* spatial resolution panchromatic (PAN) image and a *low* spatial resolution multispectral (MS) image to recover a high spatial resolution multispectral image. PAN and MS images are acquired simultaneously by an optical satellite, such as IKONOS and QuickBird. Due to physical constraints, the fusion of the PAN and MS products represents the unique solution to keep the best resolution in both domains, which might attain to less than half a meter and over eight spectral bands. The interest of the scientific community in pansharpening can be seen from the contest launched by the Data Fusion Committee of the IEEE Geoscience and Remote Sensing Society in 2006 [1] and the review papers in [2, 3]. Commercial products, see for instance Google Earth, are exploiting these synthetic images and pansharpening is becoming an important preliminary step for several image analysis tasks, see *e.g.*, change detection [4].

Most of the pansharpening papers in the literature are component substitution (CS) and Multiresolution analysis (MRA) based. The former relies upon the substitution of a component, after a spectral transformation of the MS data, with the PAN image, see *e.g.*, [5], [6], [7]. The MRA approach is based on the injection into the MS image of spatial details that are obtained from the PAN image. Laplacian pyramid [8] and "à-trous" wavelet transform [9] are usually exploited for these purposes. Approaches different from the two aforementioned classes have also been proposed. These include methods based on the Bayesian paradigm [10], total variation approaches [11], and recent developments in sparse signal representations [12].

In this paper, we extend our previous work on single image super resolution [13] to pansharpening in a variational format. We model each band of the high resolution multispectral image using a redundant basis and assume the coefficients to be sparse. We also take advantage of the linear relation between PAN and the to be recovered high spatial resolution MS image. The proposed approach is positively compared with several state-of-the-art pansharpening approaches using real data acquired by IKONOS sensor and Pléiades sensor. The remainder of the paper is organized as follows. The proposed approach is detailed in Sect. 2. Sect. 3 is devoted to the description of the experimental results. Finally, conclusions are drawn in Sect. 4.

2. THE PROPOSED METHOD

2.1. The related work

Deng *et al.* [13] proposed to use a *continuous modeling* approach to enhance image resolution from solely *one* low resolution image. The super-resolution problem is solved from an image intensity function estimation perspective. They model the intensity of the image of interest as a function defined on a *continuous* domain. To better characterize smooth component and non-smooth component such as edges of an image, two different sets of functions were used. The smooth component is assumed to lie in a space called Reproducible Kernel

Hilbert Space (RKHS) and the edges at various locations with different orientations are represented using a group of redundant approximated Heaviside functions (AHF). When the 2D thin plate spline is used, *the smooth component* is expanded using functions $\boldsymbol{\phi}_\nu(\mathbf{z})$ and $\boldsymbol{\xi}_i(\mathbf{z})$ which represent polynomial and residual terms of Taylor expansion respectively, with $\mathbf{z} = (x, y)$.

The Heaviside function (one-dimensional) is defined as $\boldsymbol{\phi}(x) = 0$ when $x < 0$ and $\boldsymbol{\phi}(x) = 1$ when $x \geq 0$, which is singular at $x = 0$ and describes a jump at $x = 0$. We usually use its smooth approximation for practical problems. In [13], the authors use the following AHF: $\boldsymbol{\psi}(x) = \frac{1}{2} + \frac{1}{\pi}\arctan(\frac{x}{\xi})$ which approximates to $\boldsymbol{\phi}(x)$ when $\xi \to 0$ and $\xi \in \mathbb{R}$ actually controls the smoothness of the AHF. The *edges* in 2D images are expanded by the approximated Heaviside function $\boldsymbol{\psi}((\cos\theta_j, \sin\theta_j) \cdot \mathbf{z} + c_k)$ which represents an edge with θ elevation from the horizontal axis at location c_k.

Let f represent the intensity function of the underlying image defined on a continuous domain. Without loss of generality, we assume the domain is $E^2 = [0, 1] \times [0, 1]$, and f can be well represented as the sum of the smooth components and the edge components. The intensity function is then $f(\mathbf{z}) = \sum_{\nu=1}^{M} \mathbf{d}_\nu \boldsymbol{\phi}_\nu(\mathbf{z}) + \sum_{i=1}^{n} \mathbf{c}_i \boldsymbol{\xi}_i(\mathbf{z}) + \sum_{j=1}^{k}\sum_{\rho=1}^{n} \boldsymbol{\omega}_j \boldsymbol{\psi}((\cos\theta_j, \sin\theta_j) \cdot \mathbf{z} + c_\rho)$ with k orientations and n pixels. Let $\mathbf{L} \in \mathbb{R}^n$ be the given vector-form low-resolution image defined on a coarse grid, the corresponding discretization for $\boldsymbol{\phi}(\cdot), \boldsymbol{\xi}(\cdot), \boldsymbol{\psi}(\cdot)$ leads to matrices $\mathbf{T}^l \in \mathbb{R}^{n\times M}$, $\mathbf{K}^l \in \mathbb{R}^{n\times n}$ and $\boldsymbol{\Psi}^l \in \mathbb{R}^{n\times m}$ $(m = k.n)$ which are obtained respectively from the 2D thin plate spline and the AHF on the coarse grid. Similarly, we can also get the matrices on a fine grid, *i.e.*, $\mathbf{T}^h \in \mathbb{R}^{\widetilde{n}\times M}$, $\mathbf{K}^h \in \mathbb{R}^{\widetilde{n}\times n}$ and $\boldsymbol{\Psi}^h \in \mathbb{R}^{\widetilde{n}\times m}$ where $\widetilde{n}$ is the pixels number of high-resolution image and $\widetilde{n} > n$.

In [13], the intensity information of the given low-resolution image defined on a coarser grid is used to estimate coefficients of the redundant "basis":

$$\min_{\mathbf{d},\mathbf{c},\boldsymbol{\beta}} \frac{1}{2n}\|\mathbf{L} - (\mathbf{T}^l\mathbf{d} + \mathbf{K}^l\mathbf{c} + \boldsymbol{\Psi}^l\boldsymbol{\beta})\|^2 + \lambda\mathbf{c}^T\mathbf{K}^l\mathbf{c} + \alpha\|\boldsymbol{\beta}\|_1, \quad (1)$$

where λ is a positive regularization parameter.

After gaining the coefficients $\mathbf{d} \in \mathbb{R}^M$, $\mathbf{c} \in \mathbb{R}^n$ and $\boldsymbol{\beta} \in \mathbb{R}^m$, it is easy to get the high-resolution image by $\mathbf{H} = \mathbf{T}^h\mathbf{d} + \mathbf{K}^h\mathbf{c} + \boldsymbol{\Psi}^h\boldsymbol{\beta}$.

In this paper, we extend the super-resolution idea based on RKHS and the approximated Heaviside functions to pansharpening.

2.2. The proposed model and its solution

Related notations: Before introducing the proposed method, it is necessary to state related notations along this paper. **a)** Low-resolution multispectral (LRMS) image: $\mathbf{MS} \in \mathbb{R}^{m_1\times n_1\times N}$ with N bands of spectral images $\mathbf{MS}_i \in \mathbb{R}^{m_1\times n_1}$, $i = 1, 2, \cdots, N$. **b)** High-resolution multispectral (HRMS) image: $\widehat{\mathbf{MS}} \in \mathbb{R}^{m_2\times n_2\times N}$ with N spectral images $\widehat{\mathbf{MS}}_i \in \mathbb{R}^{m_2\times n_2}$, $i = 1, 2, \cdots, N$, where $m_2 = s.m_1$, $n_2 = s.n_1$ with the scale factor s. In addition, $\widetilde{\mathbf{MS}} \in \mathbb{R}^{m_2\times n_2\times N}$ represents the initial upsampled multispectral image, which is generally produced by the interpolation of $\mathbf{MS}$ (here with GS method [7]). **c)** Panchromatic (PAN) image: $\mathbf{P} \in \mathbb{R}^{m_2\times n_2}$.

In our work, the proposed model mainly involves vector forms, thus in the following context we denote the above notations as vector ones, *i.e.*, $\mathbf{MS}_i \in \mathbb{R}^{m_1 n_1\times 1}$, $\widehat{\mathbf{MS}}_i \in \mathbb{R}^{m_2 n_2\times 1}$, $\widetilde{\mathbf{MS}}_i \in \mathbb{R}^{m_2 n_2\times 1}$ and $\mathbf{P} \in \mathbb{R}^{m_2 n_2\times 1}$.

Given a low resolution multispectral image $\mathbf{MS}$ and a higher resolution panchromatic image $\mathbf{P}$, the pansharpening problem is to fuse the two images together for a higher spatial resolution multispectral image $\widehat{\mathbf{MS}}$. The proposed idea is to use the same set of functions but different coefficients to expand each of the multispectral image. The low resolution and the high resolution versions only defer in evaluation grids – one is coarser and one is finer. The coefficients are computed by minimizing the following energy function:

$$\begin{aligned}\min_{\mathbf{d_i},\mathbf{c_i},\boldsymbol{\beta}_i} \frac{1}{2N_{um}} &\sum_{i=1}^{N} \|(\mathbf{T}^h\mathbf{d}_i + \mathbf{K}^h\mathbf{c}_i + \boldsymbol{\Psi}^h\boldsymbol{\beta}_i) - \widetilde{\mathbf{MS}}_i\|_2^2 \\ &+ \frac{\mu}{2}\sum_{i=1}^{N} \mathbf{c}_i^T\mathbf{K}^l\mathbf{c}_i + \frac{\lambda_1}{2}\sum_{i=1}^{N}\|\boldsymbol{\beta}_i\|_1 \\ &+ \frac{\lambda_2}{2}\|\sum_{i=1}^{N}\boldsymbol{\omega}_i(\mathbf{T}^h\mathbf{d}_i + \mathbf{K}^h\mathbf{c}_i + \boldsymbol{\Psi}^h\boldsymbol{\beta}_i) - \mathbf{P}\|_2^2,\end{aligned} \quad (2)$$

where μ, λ_1 and λ_2 are regularization parameters, $\boldsymbol{\omega}_i$ is the weight for each underlying band. N_{um} is the number of total pixels of HRMS image, $\mathbf{K}^l \in \mathbb{R}^{m_1 n_1\times m_1 n_1}$, $\mathbf{T}^h \in \mathbb{R}^{m_2 n_2\times M}$, $\mathbf{K}^h \in \mathbb{R}^{m_2 n_2\times m_1 n_1}$, $\boldsymbol{\Psi}^h \in \mathbb{R}^{m_2 n_2\times m}$. After computing the coefficients $\mathbf{d}_i$, $\mathbf{c}_i$, $\boldsymbol{\beta}_i$, $i = 1, 2, \cdots, N$, the final HRMS image can be estimated by $\widehat{\mathbf{MS}}_i = \mathbf{T}^h\mathbf{d}_i + \mathbf{K}^h\mathbf{c}_i + \boldsymbol{\Psi}^h\boldsymbol{\beta}_i$.

The proposed model (2) is equivalent to the following matrix-vector form,

$$\min_{\mathbf{x}} \frac{1}{2N_{um}}\|\mathbf{y} - \mathbf{A}\mathbf{x}\|_2^2 + \frac{\mu}{2}\|\mathbf{B}\mathbf{x}\|_2^2 + \frac{\lambda_1}{2}\|\mathbf{C}\mathbf{x}\|_1 + \frac{\lambda_2}{2}\|\mathbf{D}\mathbf{x} - \mathbf{P}\|_2^2, \quad (3)$$

where $\mathbf{y} = [\widetilde{\mathbf{MS}}_1; \widetilde{\mathbf{MS}}_2; \cdots; \widetilde{\mathbf{MS}}_N] \in \mathbb{R}^{m_2 n_2 N\times 1}$, $\mathbf{x} = [\mathbf{d}_1; \mathbf{c}_1; \boldsymbol{\beta}_1; \cdots; \mathbf{d}_N; \mathbf{c}_N; \boldsymbol{\beta}_N] \in \mathbb{R}^{(m+m_1 n_1+M)N\times 1}$, the diagonal block matrices $\mathbf{A} = \mathrm{diag}[E, E, \cdots, E]$ where $E = [\mathbf{T}^h, \mathbf{K}^h, \boldsymbol{\Psi}^h]$, $\mathbf{B} = \mathrm{diag}[F, F, \cdots, F]$ where $F = [\mathbf{0}, (\mathbf{K}^l)^{1/2}, \mathbf{0}]$, $\mathbf{C} = \mathrm{diag}[G, G, \cdots, G]$ where $G = \mathrm{diag}[\mathbf{0}, \mathbf{0}, \mathbf{I}]$ where $\mathbf{I}$ is an identity matrix,

$$\mathbf{D} = [\omega_1\mathbf{T}^h, \omega_1\mathbf{K}^h, \omega_1\boldsymbol{\Psi}^h, \cdots, \omega_N\mathbf{T}^h, \omega_N\mathbf{K}^h, \omega_N\boldsymbol{\Psi}^h].$$

After computing the coefficient $\mathbf{x}$, it is easy to estimate the final pansharpening image by $\mathbf{A}\mathbf{x}$.

The model (3) is a ℓ_1 sparsity problem that could be solved by any ℓ_1 solver such as primal-dual method [14] and

ADMM [15]. Here, we solve the model by ADMM method. The convergence of ADMM method is guaranteed by many works, e.g., [16]. Since the ℓ_1 term in the model (3) is not differentiable, we make a variable substitution $\mathbf{u} = \mathbf{Cx}$ to get the following augmented Lagrangian problem,

$$\begin{aligned}\mathcal{L}(\mathbf{x},\mathbf{u},\mathbf{b}) =& \frac{1}{2N_{um}}\|\mathbf{y}-\mathbf{Ax}\|_2^2 + \frac{\mu}{2}\|\mathbf{Bx}\|_2^2 + \frac{\lambda_2}{2}\|\mathbf{Dx}-\mathbf{P}\|_2^2 \\ &+ \frac{\lambda_1}{2}\|\mathbf{u}\|_1 + \frac{\eta}{2}\|\mathbf{u}-\mathbf{Cx}+\mathbf{b}\|_2^2,\end{aligned} \tag{4}$$

where $\mathbf{b}$ is Lagrangian multiplier with proper size, η is a positive parameter. The problem of minimizing $\mathcal{L}(\mathbf{x},\mathbf{u},\mathbf{b})$ can be solved by iteratively and alternatively solving the following step **1)** to step **3)** (denote as **ADMM-Pan**).

1) The $\mathbf{x}$-subproblem:

$$\begin{aligned}\min_{\mathbf{x}} \frac{1}{2N_{um}}\|\mathbf{y}-\mathbf{Ax}\|_2^2 + \frac{\mu}{2}\|\mathbf{Bx}\|_2^2 + \frac{\lambda_2}{2}\|\mathbf{Dx}-\mathbf{P}\|_2^2 \\ + \frac{\eta}{2}\|\mathbf{u}-\mathbf{Cx}+\mathbf{b}\|_2^2.\end{aligned} \tag{5}$$

2) The $\mathbf{u}$-subproblem:

$$\min_{\mathbf{u}} \frac{\lambda_1}{2}\|\mathbf{u}\|_1 + \frac{\eta}{2}\|\mathbf{u}-\mathbf{Cx}+\mathbf{b}\|_2^2. \tag{6}$$

3) Update $\mathbf{b}$ by: $\mathbf{b} = \mathbf{b} + (\mathbf{u} - \mathbf{Cx})$.

The $\mathbf{x}$-subproblem can be easily solved using least squares method and the $\mathbf{u}$-subproblem has a closed form solution by soft-thresholding (see more details in [13]).

Although the proposed model (3) obtains competitive results, but we can still pick up more image details from the residual image on coarse grid, which is computed by the difference between LRMS image and the degraded version of estimated HRMS image. Here, we take an iterative strategy to enhance more image details (see Algorithm 1). The final HRMS image is generated by the sum of estimated HRMS images on each iterations. Note that the "Downsample" in step 4 of Algorithm 1 is defined as the following procedure: $\widehat{\mathbf{MS}}^{(k)}$ is first filtered by a Gaussian filter matched with the modulation transfer function (MTF) and then is downscaled to the size of $\mathbf{MS}$ by "nearest" interpolation.

Algorithm 1: The summarized pansharpening method

Input: LRMS image $\mathbf{MS}$, panchromatic image $\mathbf{P}$, $\boldsymbol{\omega}_i$
Output: HRMS image $\widehat{\mathbf{MS}}^{final}$
Initialize: Set $\mathbf{MS}^{(1)} \leftarrow \mathbf{MS}$, $\mathbf{P}^{(1)} \leftarrow \mathbf{P}$
For k = 1: $\boldsymbol{\tau}$
1) Upsample $\mathbf{MS}^{(k)}$ to get $\widetilde{\mathbf{MS}}^{(k)}$ via GS method
2) Compute coefficient $\mathbf{x}$ by iterative **ADMM-Pan**
3) Compute the pansharpened image by $\widehat{\mathbf{MS}}^{(k)} = \mathbf{Ax}$
4) Downsample $\widehat{\mathbf{MS}}^{(k)}$ to coarse grid to get $\mathbf{D}_{MS}$
5) Compute residual image $\mathbf{MS}^{(k+1)}$ = $\mathbf{MS}^{(k)}$ - $\mathbf{D}_{MS}$
6) PAN residual $\mathbf{P}^{(k+1)} = \mathbf{P}^{(k)} - \sum_{i=1}^{N} \boldsymbol{\omega}_i \widehat{\mathbf{MS}}_i^{(k)}$
Endfor
7) Compute the final HRMS image:
$$\widehat{\mathbf{MS}}^{final} = \sum_{k=1}^{\boldsymbol{\tau}} \widehat{\mathbf{MS}}^{(k)}$$

3. RESULTS AND DISCUSSION

In this section, we compare the proposed method with extensive pansharpening methods on Pléiades dataset (4 bands, 256×256 pixels) and Toulouse dataset (4 bands, 512×512 pixels) that are acquired by Pléiades[1] and IKONOS sensors. The scale factor is set as 4, thus the sizes of Pléiades dataset and Toulouse dataset are 64×64 pixels and 128×128 pixels, respectively. The experiments are implemented in MATLAB(R2013b) on a computer of 16Gb RAM and Intel(R) Core(TM) CPU i5-4590: @3.30 GHz.

For the parameters in our method, we empirically set $\lambda_1 = 2.4 \times 10^{-6}$, $\lambda_2 = 1.2 \times 10^{-5}$, $\mu = 1.2 \times 10^{-7}$, $\eta = 2.4 \times 10^{-7}$, and $\boldsymbol{\tau} = 5$. Note that, fine tuning of parameters may get better results, but we unify the parameter selection to illustrate the stability of the proposed method. We apply the proposed method to image patches to reduce the computation and storage size. The patch is set to be 6×6 pixels and with 5 pixels overlap between patches. The weights $\boldsymbol{\omega}_i$ are automatically estimated by the linear regression of the multispectral image and the spatially degraded panchromatic image [17]. In addition, we employ standard indexes to estimate the performance of different methods, *i.e.*, Q4, Q, SAM, ERGAS and SCC (see [3] for detailed definitions, the larger Q4, Q and SCC and the smaller SAM and ERGAS, the better performance).

From the quantitative results in Tab. 1, it is possible to state that the proposed approach outperforms well established state-of-the-art methods. The pansharpened image generated by the proposed method performs better in terms of both spatial and spectral fidelity with respect to the reference image. This can be noticed by looking at Fig. 1 which shows visual results of the two real datasets, *i.e.*, Pléiades and Toulouse

[1] http://www.openremotesensing.net/index.php/codes/11-pansharpening

datasets. PCA, GS, ATWT, and CNMF methods introduce a relevant spectral distortion (see *e.g.*, the road of Pléiades data and the river of Toulouse data). Better performance is obtained by the multiresolution analysis (*i.e.*, MTF-GLP and MTF-GLP-HPM methods) with a relevant reduction of the spectral distortion and an enough injection of spatial details (in particular for the MTF based approach, which takes advantages of the knowledge of the sensor). Finally, we point out that even from a visual point of view, the proposed approach reaches the best performance reducing the radiometric distortion and spectral distortion with a relevant spatial enhancement.

Table 1. The quantitative comparisons of different methods. EXP [18], PCA [6], GS [7], ATWT [19], MTF-GLP [19]+[20], MTF-GLP-HPM [19]+[20], CNMF [21].

	Q4	Q	SAM	ERGAS	SCC
Pléiades Dataset					
EXP	0.7878	0.7629	4.6685	5.7915	0.6500
PCA	0.8772	0.8896	5.0484	4.4843	0.9150
GS	0.8943	0.9004	4.7790	4.0834	0.9264
ATWT	0.9585	0.9525	3.3764	2.8409	0.9305
MTF-GLP	0.9638	0.9582	3.3154	2.6900	0.9344
MTF-GLP-HPM	0.9661	0.9630	3.3328	2.5790	0.9418
CNMF	0.9513	0.9497	4.5083	3.0692	0.9399
RKHS	**0.9756**	**0.9725**	**3.0782**	**2.2628**	**0.9424**
Touluse Dataset					
EXP	0.4827	0.4787	5.2005	6.3637	0.4751
PCA	0.7732	0.7798	4.7874	4.7327	0.8915
GS	0.7733	0.7805	4.7220	4.6864	0.8963
ATWT	0.8731	0.8670	3.7897	3.6419	0.9179
MTF-GLP	0.8828	0.8766	3.7160	3.5216	0.9231
MTF-GLP-HPM	0.8878	0.8824	3.7015	3.4034	0.9288
CNMF	0.8868	0.8863	3.6128	3.2510	**0.9302**
RKHS	**0.9073**	**0.8986**	**3.4322**	**3.0412**	0.9225

4. CONCLUSIONS

In this paper we presented a variational pansharpening technique based on the image super-resolution method of Deng *et al.* [13]. The novelty of the proposed pansharpening approach is in the representation of the pansharpened image as a continuous function in which image edges are modeled as Heaviside functions and are considered to appear sparsity in the spatial domain. Experiments were conducted in order to prove the effectiveness of the proposed technique against state-of-the-art methods belonging to both the Component Substitution and MultiResolution Analysis approaches [3]. Two datasets acquired by Pléiades and IKONOS sensors were considered for the tests. The results showed that the proposed technique outperformed reference pansharpening techniques in terms of spatial and spectral fidelity with the reference image.

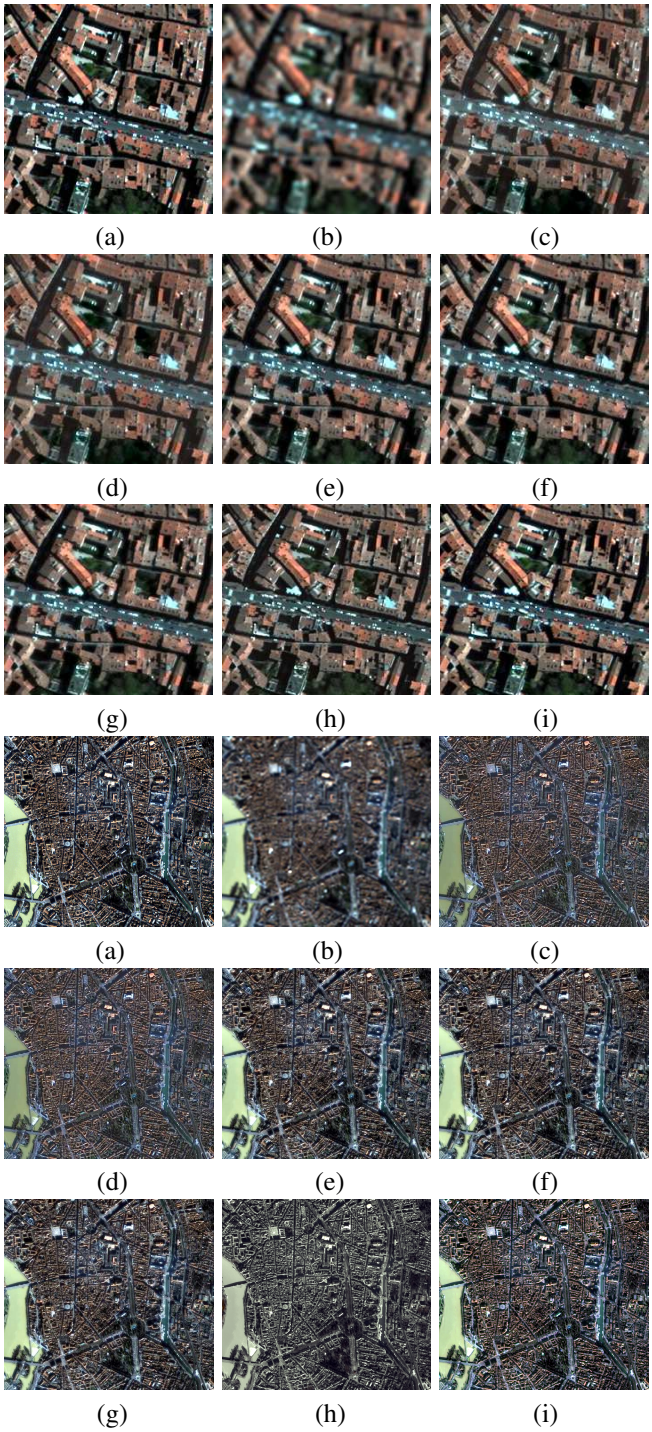

Fig. 1. First three rows for Pléiades dataset; Last three rows for Touluse dataset. (a) Reference image; (b) EXP; (c) PCA; (d) GS; (e); (f) MTF-GLP; (g) MTF-GLP-HPM; (h) CNMF; (i) Proposed.

5. ACKNOWLEDGMENT

L.-J. Deng thanks to 973 Program (2013CB329404), NSFC (61370147, 61402082) and Fundamental Research Funds for the Central Universities (ZYGX2016KYQD142), W. Guo thanks US NIH 1R21EB016535-01 and NSF DMS-1521582 for partial support, and J. Chanussot thanks to CNRS under grant PICS 263484

6. REFERENCES

[1] L. Alparone, L. Wald, J. Chanussot, C. Thomas, P. Gamba, and L. M. Bruce, "Comparison of pansharpening algorithms: Outcome of the 2006 GRS-S data fusion contest," *IEEE Transactions on Geoscience and Remote Sensing*, vol. 45, pp. 3012–3021, 2007.

[2] C. Thomas, T. Ranchin, L. Wald, and J. Chanussot, "Synthesis of multispectral images to high spatial resolution: A critical review of fusion methods based on remote sensing physics," *IEEE Transactions on Geoscience and Remote Sensing*, vol. 46, pp. 1301–1312, 2008.

[3] G. Vivone, L. Alparone, J. Chanussot, M. Dalla Mura, A. Garzelli, G. Licciardi, R. Restaino, and L. Wald, "A critical comparison among pansharpening algorithms," *IEEE Transactions on Geoscience and Remote Sensing*, vol. 53, pp. 2565–2586, 2015.

[4] C. Souza, L. Firestone, L. Silva, and D. Roberts, "Mapping forest degradation in the Eastern Amazon from SPOT 4 through spectral mixture models," *Remote Sensing of Environment*, vol. 87, pp. 494–506, 2003.

[5] P. S. Chavez Jr, S. C. Sides, and J. A. Anderson, "Comparison of three different methods to merge multiresolution and multispectral data- Landsat TM and SPOT panchromatic," *Photogrammetric Engineering and remote sensing*, vol. 57, no. 3, pp. 295–303, 1991.

[6] P. S. Chavez Jr and A. Y. Kwarteng, "Extracting spectral contrast in Landsat Thematic Mapper image data using selective principal component analysis," *Photogrammetric Engineering and Remote Sensing*, vol. 55, no. 3, pp. 339–348, 1989.

[7] C. A. Laben and B. V. Brower, "Process for enhancing the spatial resolution of multispectral imagery using pan-sharpening," 2000, US Patent 6011875.

[8] P. J. Burt and E. H. Adelson, "The Laplacian pyramid as a compact image code," *IEEE Transactions on Communications*, vol. 31, no. 4, pp. 532–540, 1983.

[9] M. J. Shensa, "The discrete wavelet transform: wedding the a trous and Mallat algorithms," *IEEE Transactions on Signal Processing*, vol. 40, no. 10, pp. 2464–2482, 1992.

[10] J. C. Price, "Combining panchromatic and multispectral imagery from dual resolution satellite instruments," *Remote sensing of environment*, vol. 21, no. 2, pp. 119–128, 1987.

[11] F. Palsson, J. R. Sveinsson, and M. O. Ulfarsson, "A new pansharpening algorithm based on total variation," *IEEE Geoscience and Remote Sensing Letters*, vol. 11, no. 1, pp. 318–322, 2014.

[12] X. X. Zhu and R. Bamler, "A sparse image fusion algorithm with application to pan-sharpening," *IEEE Transactions on Geoscience and Remote Sensing*, vol. 51, no. 5, pp. 2827–2836, 2013.

[13] L.-J. Deng, W. Guo, and T.-Z. Huang, "Single image super-resolution via an iterative reproducing kernel Hilbert space method," *IEEE Transactions on Circuits and Systems for Video Technology*, vol. 26, pp. 2001–2014, 2016.

[14] A. Chambolle and T. Pock, "A First-Order Primal-Dual Algorithm for Convex Problems with Applications to Imaging," *Journal of Mathematical Imaging and Vision*, vol. 40, pp. 120–145, 2011.

[15] B. He, M. Tao, and X. Yuan, "Alternating direction method with Gaussian back substitution for separable convex programming," *SIAM Journal on Optimization*, vol. 22, no. 2, pp. 313–340, 2012.

[16] R. Glowinski, P. L. Tallec, H. R. Sheikh, and E. P. Simoncelli, "Augmented Lagrangian and Operator Splitting Methods in Nonlinear Mechanics," *Texas*, 1989.

[17] B. Aiazzi, S. Baronti, and M. Selva, "Improving component substitution pansharpening through multivariate regression of MS+PAN data," *IEEE Transactions on Geoscience and Remote Sensing*, vol. 45, no. 10, pp. 3230–3239, 2007.

[18] B. Aiazzi, L. Alparone, S. Baronti, and A. Garzelli, "Context-driven fusion of high spatial and spectral resolution images based on oversampled multiresolution analysis," *IEEE Transactions on Geoscience and Remote Sensing*, vol. 40, pp. 2300–2312, 2002.

[19] G. Vivone, R. Restaino, M. Dalla Mura, G. Licciardi, and J. Chanussot, "Contrast and error-based fusion schemes for multispectral image pansharpening," *IEEE Geoscience and Remote Sensing Letters*, vol. 11, pp. 930–934, 2014.

[20] B. Aiazzi, L. Alparone, S. Baronti, A. Garzelli, and M. Selva, "MTF-tailored multiscale fusion of high-resolution MS and PAN imagery," *Photogrammetric Engineering & Remote Sensing*, vol. 72, no. 5, pp. 591–596, 2006.

[21] N. Yokoya, T. Yairi, and A. Iwasaki, "Coupled nonnegative matrix factorization unmixing for hyperspectral and multispectral data fusion," *IEEE Transactions on Geoscience and Remote Sensing*, vol. 50, pp. 528–537, 2012.